AIAA JOURNAL
Vol. 35, No. 1, January 1997

Two-Dimensional Focusing of Sonic Boom Noise Penetrating an Air–Water Interface

Judith L. Rochat* and Victor W. Sparrow†
Pennsylvania State University, University Park, Pennsylvania 16802

In the late 1960s and early 1970s research on supersonic aircraft determined that sonic boom noise would penetrate the surface of the ocean. It was assumed that the surface of the air–water interface was perfectly flat. Today, sonic boom noise is once again a topic of interest. The present work concentrates on two-dimensional focusing and defocusing, caused by ocean surface swell, of the penetrating sonic boom waveform. A finite difference algorithm is used to calculate the pressure levels underwater due to a rounded sonic boom waveform interacting with the water interface. Numerical results are consistent with the predictions of known theories involving 1) the existence of pressure disturbances underwater and 2) their penetration depth being a function of the aircraft's speed. These calculations also indicate that 1) the swell of the ocean surface focuses and defocuses the waveform with increasing effect as the ocean wave height increases and 2) the percent change (from a flat ocean interface to a wavy ocean interface) in pressure values due to the swell increases with increasing Mach number.

Introduction

EARLY in the next century it is expected that a new breed of supersonic passenger aircraft will be in operation over the world's oceans.[1,2] Although the parameters of the sonic booms generated by the new aircraft are unknown, it has been determined that these sonic booms will penetrate the ocean surface causing an acoustic pressure disturbance underwater. The purpose of the present research is to determine the underwater sound levels to assess the noise impact on marine life by sonic boom noise penetration into the ocean. This paper concentrates on two-dimensional focusing and defocusing, caused by the swell of the ocean surface, of the sonic boom waveform. The air and water are assumed homogeneous in the present study.

The next section of this paper offers a brief background to the current research. Following is a section covering the computational approach taken to study the problem. Next, a description of the computer program's parameters and features is given. After enumerating the specific program runs, selected results are presented. These results are qualitatively compared with known flat water theories and also provide insight into the effects of ocean surface swell on an incident sonic boom. Finally some conclusions are stated.

Background

It is well known that a supersonic aircraft creates a sonic boom when traveling faster than the speed of sound. By the time the sonic boom reaches the Earth's surface, it often approximates a plane wave N-shaped waveform. Here it is assumed that the aircraft is flying in steady flight at its cruising altitude and that atmospheric turbulence effects are negligible. It is also assumed that the incident angle at the mean ocean surface is equal to the Mach angle (at the aircraft); although a rough approximation, this is sufficient for the current research.

When an airborne plane wave interacts with a flat water surface, the sonic boom sees a large impedance change and will be totally reflected if the incident angle θ_i (angle from the normal to the water surface) is greater than 13.2 deg. If it is less than 13.2 deg, the incident plane wave creates both a transmitted propagating wave into the water and a reflected wave propagating back into the air. This critical angle of 13.2 deg corresponds to a Mach number of approximately 4.4 [$\theta_i = \theta_c = \arcsin(1/M)$, M = Mach number]. This implies that the aircraft must be traveling at a speed greater than the speed of sound in water for the sonic boom to penetrate as a propagating wave. A foreseeable speed[1–3] for a passenger supersonic aircraft would be approximately Mach 2.4, which implies the incident angle is 24.6 deg, an angle associated with total wave reflection.

Although total wave reflection occurs for speeds less than Mach 4.4, some nonpropagating sound energy does penetrate the ocean surface. Important work was done in the late 1960s and early 1970s on the study of sonic booms interacting with an air–water interface. Sawyers[4] and later Cook[5] each studied an N-shaped sonic boom interacting with a flat water surface. They analytically showed that an evanescent sound wave is produced in the water as a result of the impinging sonic boom; the amplitude of this sound wave decreases with increasing depth. A couple of years later, this theory was validated by experiments.[6–9] In 1995 Sparrow[10] showed that the penetration of these sonic booms is dependent on the aircraft speed; an evanescent sound wave penetrates further into the ocean when the incident wave is associated with a higher Mach number, even if the Mach number is less than 4.4.

The sonic boom studies mentioned here assumed that the air–water interface was perfectly flat. The ocean very rarely has a flat surface. More often than not the wind waves on the sea surface are between 1 and 2 m high. These heights correspond to wind conditions of 0–20 kn and are based on 70,000 observations.[11] The wind-generated waves of interest here are called swell; swell is defined as the waves leaving the generating area or continuing on after the generating wind has ceased.[12] An example of the swell on an ocean surface is shown in Fig. 1. The equation used to generate this curved interface is given later in this paper as Eq. (3). Although the swell depicted in Fig. 1 is simplified from an actual rough ocean surface, it allows for an analysis of the major focusing and defocusing on an incident sonic boom waveform. A study of the focusing that includes the effects of a rough surface is beyond the scope of the present research.

Among the possible methods for analyzing the interaction between a sonic boom and the assumed ocean surface, the present study chooses computational simulations. There is at least one other research group that has chosen an analytical approach.[13]

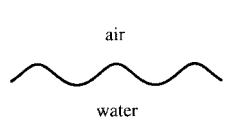

Fig. 1 Example of the shape of the ocean surface, called swell.

Presented as Paper 96-1751 at the AIAA/CEAS 2nd Aeroacoustics Conference, State College, PA, May 6–8, 1996; received May 16, 1996; revision received Sept. 16, 1996; accepted for publication Sept. 24, 1996; also published in *AIAA Journal on Disc*, Volume 2, Number 2.

*Graduate Student, Graduate Program in Acoustics.
†Associate Professor, Graduate Program in Acoustics. Member AIAA.

Method of Computational Analysis

Although a wide variety of methods exist for computational analysis, it makes sense to choose a method that is the best suited for a particular problem. Criteria can include such aspects as efficiency, accuracy, and upgradability. For this initial study, time domain finite difference methods were chosen due to their upgradability; they can be modified to model both nonlinear propagation, appropriate for very loud sonic booms, and inhomogeneous media, appropriate for turbulence in the air and bubbles in the water (probable aspects of future research).

Because of its simplicity and efficiency, a second-order two-dimensional centered finite difference scheme is used for wave propagation in the air and in the water, where the density is constant; this scheme is not implemented at the interface. Although the scheme is not a high-order method, it is very stable and has sufficient accuracy for the present problem. The centered difference scheme for the acoustic wave equation, derived from Hirsch,[14] is

$$p_{i,j}^{n+1} = 2p_{i,j}^{n} - p_{i,j}^{n-1} + c_o^2(\Delta t)^2\left[\frac{p_{i+1,j}^{n} - 2p_{i,j}^{n} + p_{i-1,j}^{n}}{(\Delta x)^2} + \left(\frac{p_{i,j+1}^{n} - p_{i,j}^{n}}{\Delta z_{j+1}} - \frac{p_{i,j}^{n} - p_{i,j-1}^{n}}{\Delta z_j}\right)\frac{2}{\Delta z_{j+1} + \Delta z_j}\right] \tag{1}$$

where the index n represents time and the indices i and j, the grid points in the x and z directions, respectively, represent space. The variable p is the acoustic pressure, c_o is the speed of sound (different for each medium, values stated later), Δt is the time increment, Δx is the spatial increment in the x direction (horizontal), and Δz is the spatial increment in the z direction (vertical). In general, $\Delta z_j = z_j - z_{j-1}$, z_j being the physical location at index j on the grid. As is indicated by Eq. (1), the computational grid must be uniform in the x direction but allows for nonuniformity in the z direction; it will be explained in the next section why this tolerance is important.

Since the air–water interface signifies a huge impedance change, it is necessary to implement a scheme capable of handling the changes in speed of sound and density. Although finite differences can easily handle the sound speed change, a factor of 4.4 between air and water, most finite difference schemes will go unstable with the huge change in ambient density, a factor of approximately 827. For example, if used alone, Eq. (1) will go unstable at the air–water interface.

To overcome this difficulty of instability, a finite difference method different than Eq. (1), similar to one used in seismology, is applied at all grid points within $\pm\frac{1}{2}\Delta z$ of the air–water interface. The scheme is derived by integrating the acoustic wave equation across the interface; this ensures proper reflection and transmission coefficients. This method was originally applied by Sochacki et al.[15] to a slightly different set of equations. The present interface finite difference scheme is written as

$$p_{i,j}^{n+1} = 2p_{i,j}^{n} - p_{i,j}^{n-1} + \frac{\Delta t^2}{a_{i,j}}\left\{\frac{1}{\Delta x^2}\left[b_{i+\frac{1}{2},j}p_{i+1,j}^{n} - \left(b_{i+\frac{1}{2},j} + b_{i-\frac{1}{2},j}\right)p_{i,j}^{n} + b_{i-\frac{1}{2},j}p_{i-1,j}^{n}\right] + \left[\frac{b_{i,j+\frac{1}{2}}(p_{i,j+1}^{n} - p_{i,j}^{n})}{\Delta z_{j+1}} - \frac{b_{i,j-\frac{1}{2}}(p_{i,j}^{n} - p_{i,j-1}^{n})}{\Delta z_j}\right] \times \frac{2}{\Delta z_{j+1} + \Delta z_j}\right\} \tag{2}$$

where p, Δt, Δx, and Δz are the same as in Eq. (1). The additional variables are $a = 1/\rho_o c_o^2$ and $b = 1/\rho_o$, ρ_o being the ambient density for each medium. Both a and b change depending on the location of the calculation. If the calculation is made in air, $c_o = 343$ m/s and $\rho_o = 1.21$ kg/m^3; if it is made in water, $c_o = 1500$ m/s and $\rho_o = 1000$ kg/m^3. However, at the interface a and b are theoretically complicated[15] and can be difficult to implement, depending on whether or not the interface line intersects grid blocks or outlines them. Because the current interface is grid block approximated (the interface line does not intersect a grid block), the functions can be written simply as $a = \frac{1}{2}(a_{\text{air}} + a_{\text{water}})$ and $b = \frac{1}{2}(b_{\text{air}} + b_{\text{water}})$.

Program Parameters and Features

There are many different variables to consider in the current problem; these include computational variables (grid parameters and boundary conditions) and physical variables (sonic boom parameters, ocean wave heights, and media).

The computational domain is a rectangular grid with hard reflecting boundaries on the left, right, and top sides and an absorbing boundary[16] on the bottom. Hard reflecting boundaries are implemented wherever possible for simplicity. Because the propagating wave starts from the upper left-hand corner of the computational domain, the left boundary is of no consequence, and reflections from the right and top boundaries would not interact with the analysis region until a time later than would cause any interference. Hard reflecting boundaries are therefore suitable for the left, right, and top sides of the domain. However, the sound speed in water is 4.4 of that in air, and false reflections from a rigid bottom boundary would interfere with the present analysis of the sound levels at the interface. Two possible solutions to avoid this interference are, first, to extend the domain by a factor of 4.4 below the water surface or, second, to implement an absorbing boundary on the bottom of the domain. The later was chosen to make the program more efficient.

The computational grid physically represents a region with dimensions 799 × 781 m (340 m in height in the air and 441 m in depth in the water); however, there are 800 grid points in both the x and z directions. This nonuniform grid has a refined region surrounding the air–water interface, a necessary feature for the program's stability. In the refined region a grid block spans 1 m in the x direction and 0.25 m in the z direction; this refined region physically extends 3 m above and 3 m below the midline of any type of ocean interface. Elsewhere in the domain, a grid block spans 1 m in the x direction and also 1 m in the z direction.

A rounded N-shaped sonic boom is inserted in the upper left-hand corner of the computational domain. Figure 2 shows a typical initial condition with a horizontal slice showing the initial rounded sonic boom waveform. The sonic boom has a specified peak pressure, duration, and angle of incidence, which, as previously mentioned, is a function of the Mach number. Using a rounded N-shaped sonic boom instead of a perfect N wave is justified for two reasons. First, realistic sonic booms vary in shape, some roughly appearing as rounded N waves; second, a perfect N wave would require a computationally intensive simulation (possibly using a very fine grid), which is not feasible at this time.

The ocean wave height is a function of the wind speed in the air; any wave height, peak to trough, can be specified. It is assumed that the wind is blowing in the x direction, and hence a two-dimensional computational analysis is appropriate. Wavelengths of these wind waves are taken to be 20 times the wind wave heights, a common ocean engineering approximation.[12] Also one of two height profiles for the curved interface can be chosen. The first type is a sinusoidal ocean surface, and the second more realistic one is a trochoidal ocean surface. Using a trochoid to represent the ocean swell was first established by Stokes[17] and improved by Rayleigh.[18] A simple expression for a Stokes' wave is provided by Khandekar[19]:

$$\eta = -A\cos kx + \tfrac{1}{2}kA^2\cos 2kx - \tfrac{3}{8}k^2A^3\cos 3kx \tag{3}$$

where η is the vertical displacement of the water surface above the mean water level, A is the wave amplitude (half the wind wave height), and k is the wave number for the ocean surface.

Even though the grid is refined in the interface region, the ocean surface curve is still approximated by ragged grid blocks; in turn, depending on the ocean wave height, the peaks and dips of the ocean waves can create numerical instabilities. To avoid this problem, a function is inserted into the Fortran code that "smooths" any peak or dip with a singular maximum or minimum grid point. Smoothing the curve requires adjusting the singular extreme point to match the value of its neighboring grid points. Again, note that the air and water are considered to be homogeneous media.

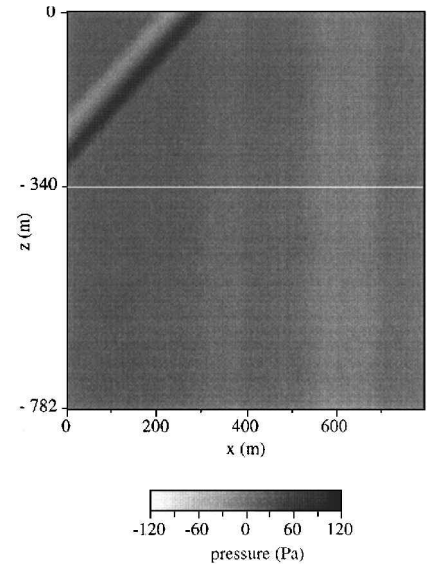

a) Full domain plot

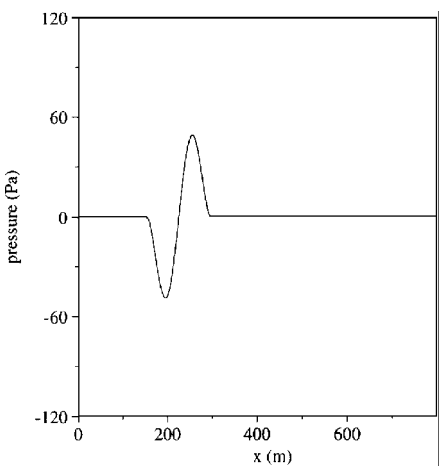

b) Horizontal line intersection

Fig. 2 Initial pulse, Mach number 1.4, wave height 0.0 m.

Calculations

A matrix of different runs changing the physical parameters were performed. In this matrix both the sonic boom and ocean parameters were varied. The Mach numbers of the fictional supersonic aircraft were chosen to be 1.4, 2.4, 3.0, and 3.5. Each initial sonic boom waveform had a peak pressure of 50 Pa and a duration of 300 ms. The four nonzero wave heights studied were 1.0, 1.4, 2.3, and 3.75 m (crest to trough); these ocean wave heights roughly correspond to wind speeds of 0, 10, 20, and 30 kn, respectively.[11] Also, runs were made using a flat water interface.

The Mach 1.4 and 2.4 cases were run for each wave height, as well as a flat surface, for both the sinusoidal and trochoidal ocean interfaces. The Mach 3.0 and 3.5 cases were run only for a flat ocean surface and for trochoidal waves at a height of 3.75 m. All runs were made on a Digital Equipment Corp. Alpha 3000/600 workstation, and each simulation took approximately 1.5–5.5 h of run time, depending on the user load.

Results

Results were obtained that are consistent with previously published results and that also show the effects of ocean swell on the penetrating sonic boom noise.

When viewing Figs. 2a, 3a, and 5a, the plot is stretched in the region corresponding to the refined grid region in the computational domain. As previously mentioned, the refined region extends 3 m both above and below the midline of the air–water interface. The figures show every grid point as a pixel, and so the 6 m of the refined region is shown as 24 m in height. In other words, the unrefined 1-m height computational grid blocks still correspond to 1 m in the figures, but the refined 0.25-m height grid blocks now also correspond to 1 m.

Comparison with Known Results

The analytical theories of Sawyers,[4] Cook,[5] and Sparrow[10] assume a flat water interface. The finite difference simulation results for the flat ocean interface can be qualitatively compared with these analytical theories. Although the finite difference simulations use a rounded sonic boom waveform and the analytical theories assume a perfectly N-shaped waveform, the finite difference results are similar to those predicted analytically. An example of a flat water image can be seen in Fig. 2. Figure 2a shows the initial Mach 1.4 waveform in the computational domain, and Fig. 2b shows a horizontal slice through this waveform. The amplitude of this pressure waveform is approximately 50 Pa.

When the sonic boom interacts with the ocean surface, an evanescent wave is produced underwater. Line graphs extracted at various depths below the surface illustrate the decaying waveform as described by both Sawyers and Cook. Figure 3a, a snapshot at time $t = 0.79$ s for the Mach 1.4 flat ocean surface run, illustrates the incident wave interacting with the air–water interface; Fig. 3b shows a horizontal line intersection of the waveform just under the ocean surface and at 10, 25, and 50 m underwater. The pressure amplitude just under the ocean surface is approximately 100 Pa due to

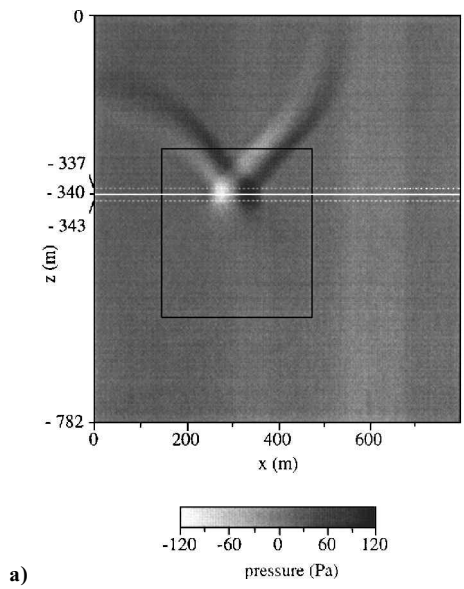

a)

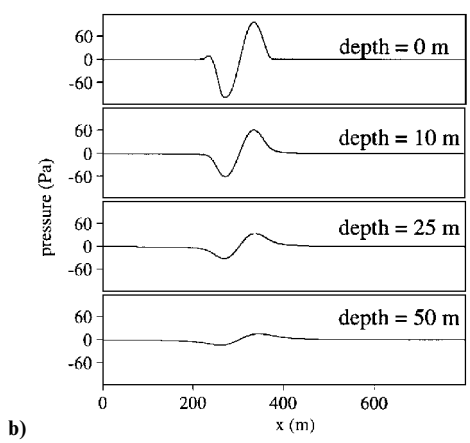

b)

Fig. 3 Mach number 1.4, wave height 0.0 m; incident wave interacting with the interface: a) full domain plot, boxed region signifying the data from which the results are extracted and b) horizontal line intersection of waveform just under the water surface and 10, 25, and 50 m underwater.

Table 1 Real pressure values found at 100-m depth for increasing Mach numbers

Mach no.	Positive peak, p, Pa	Negative peak, p, Pa
1.4	4.19	−5.71
2.4	14.06	−15.98
3.0	21.71	−24.96
3.5	40.71	−38.20

Table 2 Percent change in peak pressure from the flat ocean results due to focusing and defocusing caused by ocean swell (trochoidal waves)

Wind wave height (crest to trough), m	Change in +/− pressure peaks due to curvature effects, % $M = 1.4$	$M = 2.4$
0	0/0	0/0
1.0	−0.4/−0.1	0.4/0.6
1.4	0.8/0.5	1.7/−0.7
2.3	1.5/2.4	−2.8/−2.8
	−1.4/2.5	4.2/5.3
3.75	0.1/−3.4	−5.4/11.7
	1.3/5.0	7.8/−8.9

pressure doubling at the air–water interface. Figure 3 does, in fact, show that the amplitude of the penetrating wave decays as a function of depth. The frequency dependence of this decaying waveform was previously investigated.[20]

The black box in Fig. 3a (also in Fig. 5a) represents a region of the full computational domain from where all results are extracted. Because of the finite speeds of sound in the full domain (i.e., causality), one can ignore the part of the domain outside the black box. This outside part of the domain is obviously affected by the chosen initial and boundary conditions, and the results there are not usable.

To see the relationship between Mach number and the underwater depth of the penetrating sound, it is necessary to extract information from the flat water Mach 1.4, 2.4, 3.0, and 3.5 runs. Table 1 contains the numerical data, the real pressure values, found at a 100-m depth for increasing Mach numbers. It is seen that at Mach 1.4 the evanescent wave has decayed to less than 2.5% of its value just under the ocean surface (100 Pa). However, for Mach 3.5 the peak pressures in the waveform at a depth of 100 m are still 40% of the value just under the surface. Hence, the numbers confirm Sparrow's prediction,[10] which states that higher Mach number incident waves are associated with deeper penetration into the ocean.

Effects Caused by Ocean Swell

The effects caused by a sonic boom interacting with an ocean interface with swell can be divided into two main categories: 1) how different wind wave heights strengthen the focusing and defocusing of the evanescent acoustic pressure and 2) how different Mach numbers strengthen the focusing and defocusing. In addition to still image results, an interesting observation is made from animating the results.

For the first category, numerical results were extracted from the Mach 1.4 and 2.4 runs for all wave heights. Table 2 contains typical percentage values reflecting the change in positive and negative peaks (in the pressure waveform just under the ocean surface) from the flat ocean result to each wavy ocean result. These numbers are taken from the trochoidal interface calculations; the trochoidal and sinusoidal interfaces yielded such similar results that it is sufficient to present just the one case.

Over the time it takes for the sonic boom to finish interacting with the ocean, the positive and negative peaks of the waveform have each interacted with several crests and troughs of the ocean surface swell. For Table 2, each set of positive and negative peak percent changes is calculated from the numerical pressure values at a single time during the wave propagation simulation. Different snapshots in time are examined to determine typical percent change values. Depending on where on the curved interface the sonic boom wave is incident, the peak pressure values just under the surface may be either increased or decreased by varying amounts. Because

Table 3 Percent change in peak pressure from the flat ocean results due to focusing and defocusing caused by ocean swell (trochoidal waves)

Wind wave height (crest to trough), m	Change in +/− pressure peaks due to curvature effects, % $M = 1.4$	$M = 2.4$	$M = 3.0$	$M = 3.5$
0	0/0	0/0	0/0	0/0
3.75	1.3/5.0	−5.4/11.7	5.1/15.4	8.6/16.9

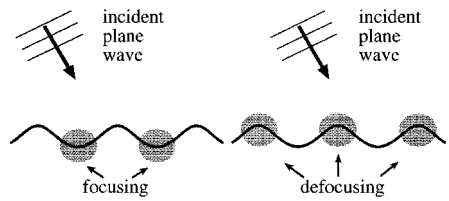

Fig. 4 Focusing and defocusing of a wave incident on an ocean surface with swell. The shaded regions represent the regions of focusing and defocusing. This picture is not intended to illustrate a sonic boom interacting with the ocean surface but rather just to show where focusing and defocusing occurs.

the percentage increase or decrease varies considerably for the 2.3- and 3.75-m wind wave heights, two typical results are shown for each. Figure 4 illustrates what is meant by focusing (which causes an increase in amplitude) and defocusing (which causes a decrease in amplitude) of the incident wave.

The percent change values in Table 2 indicate that for larger ocean wave heights the pressure values are more affected, either being decreased or increased. For a calm ocean (wave height being 1 m), the deviation in peak pressure from the perfectly flat ocean result is less than 1%, whereas for an ocean with significant swell (wave height being 3.75 m), changes can be large as 5 or 11%.

An example of a waveform changed by the interface curvature is shown in Fig. 5. The case shown is Mach 2.4 at time $t = 0.75$ s with the wave height being 3.75 m; this corresponds to the −5.4/11.7% case in Table 2. Figure 5a shows the full domain, and Fig. 5b shows a horizontal line intersection taken in the water close to the surface; the solid line represents the horizontal intersection for the case involving the ocean wave height of 3.75 m and the dashed line (plotted for comparison) represents the case involving the flat ocean surface. Similar to Fig. 3b, the amplitudes of the waveforms in Fig. 5b are much higher than that in Fig. 2b, the initial waveform before hitting the ocean surface, due to pressure doubling at the air–water interface; the initial waveform's peak pressure is 50 Pa and the amplitude of the dashed line waveform in Fig. 5b is 100 Pa. The solid line waveform in Fig. 5b looks slightly distorted due to the curvature effects. Again, note that the picture of the full domain is stretched in the interface region.

For the second category (how different Mach numbers strengthen the focusing and defocusing), runs including all Mach numbers but just the most extreme trochoidal wave height, 3.75 m, were evaluated. Table 3 shows the percent changes in pressure values just under the ocean surface (from an incident plane wave interacting with a flat surface to one interacting with a wavy surface). Only cases with the greatest percent changes are shown. In viewing the data in Table 3, it can be seen that the highest percent changes increase with increasing Mach number.

An animation of the Mach 2.4/wave height 3.75 m/trochoidal interface profile simulated data was created as a research tool. Observing this animation, it was seen that the positive and negative peak of the rounded sonic boom waveform just above the ocean surface became increased (in magnitude) in the troughs of the ocean waves and decreased (in magnitude) over the ocean wave crests. The highest pressure values were located near the bottom of the trough and up the right-hand side slope of the trough. Recall that the airborne sonic boom is traveling from left to right over the ocean surface.

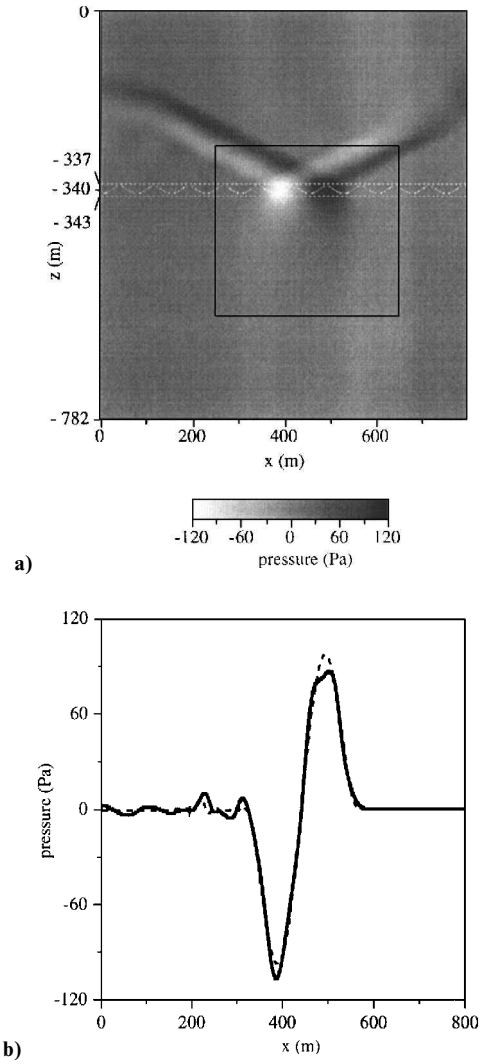

Fig. 5 Mach number 2.4, wave height 3.75 m incident wave interacting with the interface: a) full domain plot, boxed region signifying the data from which the results are extracted and b) horizontal line intersection of waveform just under the water surface; 3.75 m wave height case (solid line), flat interface case (dashed line).

Conclusions

Through the use of computational simulation, penetrating underwater pressure values caused by a rounded N-shaped sonic boom interacting with a simplified ocean surface have been predicted. Several parameters were varied to see trends in the numerical data; these included Mach number, ocean wave height, and ocean wave shape. The results support the known analytical theories for a flat ocean surface: 1) an evanescent wave underwater is created by an impinging sonic boom for Mach numbers below 4.4 and 2) the penetration depth is a function of Mach number (larger Mach numbers imply deeper penetration). The results also indicate that 1) ocean surface swell focuses and defocuses the waveform with increasing effects as the ocean wind wave height increases and 2) the percent change in peak acoustic pressure values due to the swell increases with increasing Mach number. Observations using animations indicate that pressure values due to the sonic boom are increased (in magnitude) in the troughs of the ocean wind waves.

As was mentioned earlier, the results presented here assume that the wind waves are aligned in the same direction as is the propagating sonic boom. Studies remain to be conducted that are fully three-dimensional where the wind waves and propagating sonic boom are not aligned. It was further assumed that the air and water were both homogeneous. Since in a realistic ocean many air bubbles exist near the surface, improved predictions would include these inhomogeneities, which can cause a significant change in the apparent characteristic impedance seen by an incident sonic boom at the air–water interface.

Acknowledgments

The authors appreciate financial support from NASA Langley Research Center Grant NAG-1-1638, administered by Gerry L. McAninch.

References

[1]Poisson-Quinton, P., "Future SSTs, A European Approach," *Aerospace America*, Vol. 32, No. 9, 1994, pp. 39–43.

[2]Williams, L. J., "HSCT Research Gathers Speed," *Aerospace America*, Vol. 33, No. 4, 1995, pp. 32–37.

[3]Vartabedian, R., "Launching Supersonic Dreams," *Los Angeles Times*, June 1, 1994.

[4]Sawyers, K. N., "Underwater Sound Pressure from Sonic Booms," *Journal of the Acoustical Society of America*, Vol. 44, No. 2, 1968, pp. 523, 524.

[5]Cook, R. K., "Penetration of a Sonic Boom into Water," *Journal of the Acoustical Society of America*, Vol. 47, No. 5, Pt. 2, 1970, pp. 1430–1436.

[6]Intrieri, P., and Malcolm, G., "Ballistic Range Investigation of Sonic-Boom Overpressures in Water," *AIAA Journal*, Vol. 11, No. 4, 1973, pp. 510–516.

[7]Malcolm, G., and Intrieri, P., "Ballistic Range Investigation of Sonic-Boom Overpressures in Water," AIAA Paper 72-657, June 1972.

[8]Waters, J., "Penetration of Sonic Boom Energy into the Ocean: An Experimental Simulation," *Noise and Vibration Control Engineering*, edited by M. Crocker, Proceedings of the Purdue Noise Control Conf., 1971, pp. 554–557.

[9]Waters, J., and Glass, R. E., "Penetration of Sonic Boom Energy into the Ocean: An Experimental Simulation," Hydrospace Research Corp., Final Rept. on Contract FA70-WAI-185, HRC TR 288, June 1970; available from National Technical Information Service, Springfield, VA, as AD 711 963.

[10]Sparrow, V. W., "The Effect of Supersonic Aircraft on the Penetration of Sonic Boom Noise into the Ocean," *Journal of the Acoustical Society of America*, Vol. 97, No. 1, 1995, pp. 159–162.

[11]Bascomb, W., *Waves and Beaches*, Anchor, New York, 1980, p. 48.

[12]Gaythwaite, J., *The Marine Environment and Structural Design*, Van Nostrand Reinhold, New York, 1981, p. 61.

[13]Cheng, H. K., Lee, C. J., Hafez, M. M., and Guo, W. H., "Sonic Boom Propagation and Its Submarine Impact: A Study of Theoretical and Computational Issues," AIAA Paper 96-0755, Jan. 1996.

[14]Hirsch, C., *Numerical Computation of Internal and External Flows: Volume 1: Fundamentals of Numerical Discretization*, Wiley, New York, 1988, Chap. 4.

[15]Sochacki, J. S., George, J. H., Ewing, R. E., and Smithson, S. B., "Interface Conditions for Acoustic and Elastic Wave Propagation," *Geophysics*, Vol. 56, No. 2, 1991, pp. 168–181.

[16]Sparrow, V. W., and Raspet, R., "Absorbing Boundary Conditions for a Spherical Monopole in a Set of Two-Dimensional Acoustics Equations," *Journal of the Acoustical Society of America*, Vol. 87, No. 6, 1990, pp. 2422–2427.

[17]Stokes, G. G., "Supplement to a Paper on the Theory of Oscillatory Waves," *Math. and Phys. Pap.*, Vol. 1, Cambridge Univ. Press, Cambridge, England, UK, 1880, pp. 314–326.

[18]Rayleigh, J. W. S., "Hydrodynamical Notes," *Philosophical Magazine*, Vol. 21, 1911, pp. 177–195.

[19]Khandekar, M. L., *Operational Analysis and Prediction of Ocean Wind Waves*, Springer–Verlag, New York, 1989, p. 21.

[20]Rochat, J. L., and Sparrow, V. W., "Sound Levels Under the Ocean Surface due to Sonic Boom Penetration," *Proceedings of Inter-Noise 95*, Noise Control Foundation, New York, 1995, pp. 967–970.